

---

# A Computational Analysis Based on Automatic Digitization of Movement Tracks Reveals the Altered Diurnal Behavior of the Western Flower Thrips, *Frankliniella occidentalis*, Suppressed in PKG Expression

---

[Chunlei Xia](#) , Gahyeon Jin , [Falguni Khan](#) , [Hye-Won Kim](#) , Yong-Hyeok Jang , Nam Jung , [Yonggyun Kim](#) <sup>\*</sup> , [Tae-Soo Chon](#) <sup>\*</sup>

Posted Date: 7 February 2025

doi: 10.20944/preprints202502.0453.v1

Keywords: Diurnal behavior; Neural network; Thrips; PKG; RNA interference



Preprints.org is a free multidisciplinary platform providing preprint service that is dedicated to making early versions of research outputs permanently available and citable. Preprints posted at Preprints.org appear in Web of Science, Crossref, Google Scholar, Scilit, Europe PMC.

Copyright: This open access article is published under a Creative Commons CC BY 4.0 license, which permit the free download, distribution, and reuse, provided that the author and preprint are cited in any reuse.

Article

# A Computational Analysis Based on Automatic Digitization of Movement Tracks Reveals the Altered Diurnal Behavior of the Western Flower Thrips, *Frankliniella occidentalis*, Suppressed in *PKG* Expression

Chunlei Xia <sup>1,2</sup>, Gahyeon Jin <sup>3</sup>, Falguni Khan <sup>3</sup>, Hye-Won Kim <sup>1,4</sup>, Yong-Hyeok Jang <sup>1</sup>, Nam Jung <sup>1,2</sup>, Yonggyun Kim <sup>3,\*</sup> and Tae-Soo Chon <sup>1,2,\*</sup>

<sup>1</sup> Research and Development, Ecology and Future Research Institute (EnFRI), Busan

<sup>2</sup> Research Institute of Computer, Information and Communication, Pusan National University, Busan

<sup>3</sup> Department of Plant Medicals, Andong National University, Andong 36729, Korea

<sup>4</sup> Department of Electrical and Electronics Engineering, Pusan National University, Busan

\* Correspondence: hosanna@anu.ac.kr (Y.K.); tschon.chon@gmail.com (T.C.)

**Simple Summary:** Diurnal behavior is a character of the western flower thrips, *Frankliniella occidentalis*. It is controlled by the circadian clock machinery of the thrips. However, it was unclear how the clock machinery controls the diurnal behaviors such as feeding or mating. This study hypothesized that a foraging gene encoding cGMP-dependent protein kinase (*PKG*) mediates the diurnal behaviors. RNA interference of *PKG* expression led to significant alteration of clock gene expression and gave adverse effects on immature development and adult fecundity. To examine the behavioral alteration, adult movement was continuously observed for 24 h-period with an automatic digitization device. Diel difference was observed with speed and durations (%) in RNAi-control females but not in the RNAi-treated females. Three sequential stages consisting of high activity followed by feeding and visiting to micro-areas were observed for the control females but not in the RNAi-treated females. These results suggest that *PKG* mediates the diurnal behavior of *F. occidentalis* under the control of the circadian clock machinery.

**Abstract:** The western flower thrips, *Frankliniella occidentalis*, a worldwide insect pest with its polyphagous feeding behavior and transmitting virus, follows a diurnal rhythmicity driven by expression of the circadian clock genes. However, it remained unclear how the clock signal triggers the thrips behaviors. This study posed a hypothesis that the clock signal modulates cGMP-dependent protein kinase (*PKG*) activity to mediate the diurnal behaviors. A *PKG* gene is encoded in *F. occidentalis* and exhibits high sequence homologies with those of honeybee and fruit fly. Interestingly, its expression followed a diel pattern with high expression during photophase in larvae and adults of *F. occidentalis*. It is noteworthy that *PKG* expression was clearly observed in the midgut during photophase but not in scotophase from our fluorescence *in situ* hybridization analysis. A prediction of protein-protein interaction suggested its functional association with clock genes. To test this functional link, RNA interference (RNAi) of the gene expression was performed by feeding a gene-specific double stranded RNA and led to significant alteration of the two clock genes (*Clock* and *Period*) in their expression levels. The RNAi treatment gave adverse effects on immature development and adult fecundity. To further analyze the role of *PKG* in implementing the diurnal behavior, the adult females was continuously observed for 24 h-period with an automatic digitization device to obtain movement parameters and durations (%) in different micro-areas in the observation arena. Diel difference was observed with speed in RNAi-control females at 0.16 mm/s and 0.08 mm/s, in photo- and scoto-phase, respectively, whereas diel difference was not observed for the *PKG*-specific RNAi-treated females by showing 0.07 mm/s and 0.06 mm/s, respectively. The diel difference was also observed in durations (%) in the control females, more strongly in the intermediate area in the

observation arena. Speed and durations in the different micro-areas in mid-scotophase were significantly different from most photophase in the control females, while speed was significantly different mainly during late photophase in comparing effects of control and RNAi treatments in each light phase. Three sequential stages consisting of high activity followed by feeding and visiting to micro-areas were observed for the control females. For RNAi-treated females the three phases were disturbed with irregular speed and visits to micro-areas. These results suggest that PKG is associated with implementing the diurnal behavior of *F. occidentalis* under the oscillating expressions of the clock genes.

**Keywords:** diurnal behavior; neural network; thrips; PKG; RNA interference

---

## 1. Introduction

The western flower thrips, *Frankliniella occidentalis*, is polyphagous and gives a feeding damage to high-value crops including hot peppers [1]. The insect pest also transmits plant virus to crops, causing a devastating economic damage [2]. Due to frequent use of chemical insecticides, this species develops insecticide resistance [3]. Moreover, its hiding behavior into flowers or crevices makes it difficult to be effectively controlled by the insecticide sprays [4]. Alternatively, non-chemical control techniques have been developed and implemented to suppress the outbreaks of *F. occidentalis*. For example, aggregation pheromone has been used to sticky trap for mass-trapping [5,6]. In addition to chemical cues, the visual signals during day time are useful to locate hosts of the thrips under the diurnal feeding and mating rhythmicity [7,8]. Four circadian clock genes (Period (*Per*), Timeless (*TIM*), Doubletime (*DBT*), and Clock (*CLK*)) are expressed in *F. occidentalis* and associated with the diel rhythmicity [8].

Insect feeding behavior is functionally associated with expression of a *foraging* gene encoding a cGMP-dependent protein kinase (*PKG*) [9]. Upon activation by cGMP, PKG phosphorylates a number of biologically important targets associated with the regulation of muscle contraction, metabolism, and gene expression [10]. Variation of *PKG* expression is implicated in plasticity of insect behaviors [11]. Manipulation of its expression level and subsequent kinetic activity influence on alternative feeding behaviors of the fruit fly, *Drosophila melanogaster* called sitters and rovers around diet [12]. The expression levels also drive division of labor systems across diverse social species [13,14]. These suggest a functional role of PKG in controlling insect behaviors. In mammals, the circadian clock is entrained depending on the onset of light signal by PKG activity, which is induced by cGMP up-regulated by nitric oxide (NO) and catalyzes the phosphorylation of TIM [15]. This suggests that PKG influences on the circadian clock of *F. occidentalis*. However, the function link between PKG and circadian clock remained elusive in insects.

This study investigated the physiological role of PKG in the diurnal behavior of the thrips, *F. occidentalis*, by regulating expression of the clock genes. To address this hypothesis, this study predicted PKG gene in *F. occidentalis* and its expression levels were monitored during 24-h period. To test the functional link, *PKG* expression was suppressed by its specific RNA interference (RNAi) and the resulting changes of the clock gene expressions were analyzed. In addition, any subtle alteration of the thrips behavior was assessed by mathematical parameters extracted from automatically detected data of the movement tracks by a continuous 24 h-monitoring device.

## 2. Materials and Methods

### 2.1. Insect Rearing

Both larvae and adults of *F. occidentalis* were obtained from the Department of Crop Protection, National Institute of Agricultural Sciences (Jeonju, Korea), and maintained at conditions of  $25 \pm 1^\circ\text{C}$  temperature,  $60 \pm 5\%$  relative humidity, and a 14:10 h (L:D) light cycle. Newly germinated beans (*Phaseolus coccineus* L.) were supplied for feeding and oviposition. Eggs that were newly laid on the beans in adult colonies were transferred to the breeding dish (SPL Life Science, Seoul, Korea). After 3 days, at which point most larvae hatched, new beans were supplied every day. Under the laboratory conditions, larvae underwent two instars (L1 - L2) and were distinct from prepupae or pupae that developed wing pads.

### 2.2. Bioinformatics Analysis

DNA and amino acid sequences including *PKG* gene of *F. occidentalis* (*Fo-PKG*) were obtained from NCBI (National Center for Biotechnology Information: <https://blast.ncbi.nlm.nih.gov>) with accession numbers. MEGA6.0 was used to construct a phylogenetic tree through clustering using Maximum likelihood, where the evolutionary distances were computed using the Poisson correction method. Bootstrapping values were obtained with 1,000 trials to support branching and clustering. Protein domains were predicted using a program searching the conserved domain (<https://www.ncbi.nlm.nih.gov/Structure/cdd/wrpsb.cgi>), and InterPro (<https://www.ebi.ac.uk/interpro/>). The N-terminal signal peptide was determined using SignalP 5.0 server (<https://services.healthtech.dtu.dk/service.SignalP-5.0/>). The resulting domains were drawn by Biorender (<https://biorender.com/>). Protein-protein interaction map was generated by using STRING 12.0 (<https://string-db.org>)

### 2.3. RNA Extraction and cDNA Preparation

Total RNAs were extracted using Trizol reagent (Invitrogen, Carlsbad, CA, USA) according to the manufacturer's protocol. For each RNA extraction, 25 females were macerated using 500  $\mu\text{L}$  of Trizol reagent. Following the RNA extraction, RNA was resuspended in 30  $\mu\text{L}$  of diethylpyrocarbonate (DEPC)-treated water and quantified using a spectrophotometer (Nanodrop, Thermo Fisher Scientific, Wilmington, DE, USA). For cDNA synthesis, 400 ng of RNA was used in each sample with RT oligo dT premix (Intron Biotechnology, Seoul, Korea) containing oligo dT primer. A reaction mixture consisted of 2  $\mu\text{L}$  of RNA extract and 18  $\mu\text{L}$  of DEPC-treated water and was run according to the manufacturer's instructions. The resulting cDNA samples were kept at  $-20^\circ\text{C}$  before being used for experimentation.

### 2.4. RT-PCR and RT-qPCR

RT-PCR used the cDNA and amplified *Fo-PKG* and two clock genes with a Taq polymerase (GeneALL, Seoul, Korea). A reaction mixture for PCR consisted of 2.5  $\mu\text{L}$  of dNTP (each 10 pmol), 2.5  $\mu\text{L}$  of  $10\times$  Taq buffer, 2  $\mu\text{L}$  of forward and reverse primers (10 pmol/ $\mu\text{L}$ , Table S1), 0.5  $\mu\text{L}$  of Taq polymerase, 1  $\mu\text{L}$  of cDNA, and 16.5  $\mu\text{L}$  of distilled deionized water. The PCR conditions began with an initial denaturation at  $95^\circ\text{C}$  for 5 min, which was followed by 35 amplification cycles consisting of  $95^\circ\text{C}$  for 1 min,  $50 \sim 55^\circ\text{C}$  for 30 sec, and  $72^\circ\text{C}$  for 1 min. At the end of the amplification cycle, an additional extension was performed at  $72^\circ\text{C}$  for 5 min. The PCR product was confirmed by 1% agarose gel electrophoresis. The qPCR used a Step One Plus Real-Time PCR System (Applied Biosystem) under the guidelines of Bustin et al. [16]. A sample of qPCR reaction (20  $\mu\text{L}$ ) contained 10  $\mu\text{L}$  of Power SYBR Green PCR Master Mix (Toyobo, Osaka, Japan), 3  $\mu\text{L}$  of cDNA template (100 ng), and 1  $\mu\text{L}$  (10 pmol) each of the forward and reverse primers (Table S1). After an initial heat treatment at  $95^\circ\text{C}$  for 2 min, qPCR was performed with 40 cycles of denaturation at  $95^\circ\text{C}$  for 30 s, annealing at  $50\sim 55^\circ\text{C}$  for 30 s, and extension at  $72^\circ\text{C}$  for 30 s. The transcript levels of elongation factor

1 (EF1) were used as a reference for the normalization of each test sample. Quantitative analysis was conducted using the comparative CT ( $2^{-\Delta\Delta CT}$ ) method [17]. All experiments were independently replicated three times.

### 2.5. RNA Interference (RNAi) Treatment and Subsequent Behavior Assays

Template DNA was amplified with gene-specific primers (Table S1) containing T7 promoter sequence (5'-TAATACGACTCACTATAGGGAGA-3') at the 5' end. The PCR conditions were as described above. After confirming the PCR product, the resulting PCR product was used to synthesize double-stranded RNA (dsRNA) encoding Fo-PKG using T7 RNA polymerase with NTP mixture at 37°C for 3 h (MEGA script RNAi kit, Ambion, Austin, TX, USA). dsRNA (2 µg/10 µL) specific to Fo-PKG ('dsPKG') was mixed with a transfection reagent Metafectene PRO (Biontex, Plannegg, Germany) at a 1:1 (v/v) ratio and incubated at 25°C for 30 min to form liposomes, and the resulting mixture was supplied with bean to *F. occidentalis*. Bean was coated with the dsRNA mixture of 10 µL per 20 thrips and fed for 12 h. Control dsRNA ('dsCON') was prepared according to the method outlined by Vatanparast et al. [18].

### 2.6. Fluorescence In Situ Hybridization (FISH) Assay

Adult thrips were tested using FISH assay to detect the expression pattern of Fo-PKG. The guts of thrips were dissected upon a sterilized glass slide and then treated with 4% paraformaldehyde for 1 h at room temperature. The guts were permeabilized with 1% Triton X-100 in PBS for 2 h at room temperature after being cleaned with 1× PBS. After that, the gut was washed with 1× PBS, rinsed with 2× SSC, and incubated for 1 h at 42°C in a dark, humid environment with 25 µL of pre-hybridization solution (2 µL of yeast tRNA, 2 µL of 20× SSC, 4 µL of dextran sulfate, 2.5 µL of 10% SDS, and 14.5 µL of deionized distilled water). The buffer was then replaced with hybridization buffer (5 µL of deionized formamide and 1 µL of oligonucleotide (10 pmol) tagged with fluorescein in 19 µL of the pre-hybridization buffer). The DNA oligonucleotide probes were tagged with fluorescein amidite (FAM) at the 5' end and purified using high performance liquid chromatography at Bioneer (Daejeon, Korea). To identify Fo-PKG mRNA, an antisense probe (5'-FAM-TTT-TCAGTCACATTGTGTACGTT-3') that is complementary to the target mRNA and a negative dsCON sense probe (5'-FAM-AAA-AACGTACACAATGTGACTGA-3') were produced at a concentration of 10 pmol. The slides were then sealed with an RNase-free coverslip and left in a humidity room at 42°C for 16~18 h. Following hybridization, the gut was incubated with 4× SSC containing 1% Triton X-100 at room temperature for 5 min, and it was rinsed twice with 4× SSC for 10 min each. The gut samples were washed three times with 4× SSC and then incubated at 37°C with a 1% solution of anti-rabbit-FITC conjugated antibody (Thermo Fisher Scientific) in PBS for 30 min under darkness. The guts were incubated with 4× SSC for 10 min, and then with 2× SSC for 10 min. The samples were viewed under a fluorescence microscope (DM2500, Leica, Wetzlar, Germany) at 200× magnification after adding a drop of PBS/glycerol (1:1, v/v) and incubating at room temperature for 15 min.

### 2.7. Behavior-Monitoring and Automatic Digitization

Individual adult female thrips at 2-3 days after emergence were observed continuously for 24 h in each trial. The detailed observation system is provided in Supplementary information 2. Observation system was installed on an optic fiber microscope (Camscope®, AST-ICS305B, Somotech Vision, Seoul, Korea) consisting of observation arena, camera, computer, and light (Figure S1A). The observation arena (6 mm in diameter and 1.7 mm in depth) was made of dental modelling wax [19] and was divided into food-provision (2.5 mm radius), intermediate (0.5 mm width) and edge (1 mm width) areas (Figure S1B). Within the food-provision area, a particle (2 mm in diameter and 1 mm in height) of fresh bean just after germination was provided as food in the center. Water was provided for the food continuously to keep the food fresh during the observation period (Figure S1C).

Temperature was  $23.6 \pm 2.0^\circ\text{C}$  and humidity was  $55.3 \pm 10.0\%$  in the observation room. Photophase (14 L) and scotophase (10D) were provided with white and red LEDs, respectively. In order not to cause compound effects between transplant of test females and light phase change, the test females were introduced to the observation arena 2 h before the start of photophase for acclimation. Digital observation was conducted continuously for 24 h just after light-on in the light cycle.

Behavioral tracks were recorded with an image resolution of  $1,920 \times 1,080$  with 15.88 frames per second (fps). Movement was recognized by a convolutional neural network, YOLOv8 [20] continuously in photo- and scoto-phases as examples shown in Figure S1D. One second was defined as observation time unit to obtain movement parameters and duration rates in percentage (durations (%)) in this study, although time intervals of less than 1 s (e.g., 0.25 s) have been used in similar research to monitor the movement of insects (e.g., *Drosophila melanogaster*) responding to external stimuli (toxins) [21–23]. Measuring the parameters at a time interval of 1 s was sufficient to present the movement and positioning status over the entire 24 h period. The time unit in 1 s also reduced the computational time.

Speed, locomotory rate, and direction change rate (DCR) were recorded for movement parameters, while durations (%) in different micro-areas were obtained to present where test animals stayed within the observation arena as time progressed. Whereas speed was obtained over the entire observation period including the time without movement, locomotory rate was defined as the mean speed only when the test individuals moved. DCR was calculated as the angle change (without considering direction) after one unit time (1 s). Duration of staying at the food-provision (edge) area was measured as the total period while the digitized body center was located either within or on the border of food-provision (edge area). The rest of the period was regarded as duration in the intermediate area. The parameters and durations (%) were measured in each time unit first, and averaged in each hour defined as a light phase (i.e., P1, ..., P14 for photophase, and S1, ..., S10 for scotophase).

## 2.8. Statistical Analysis

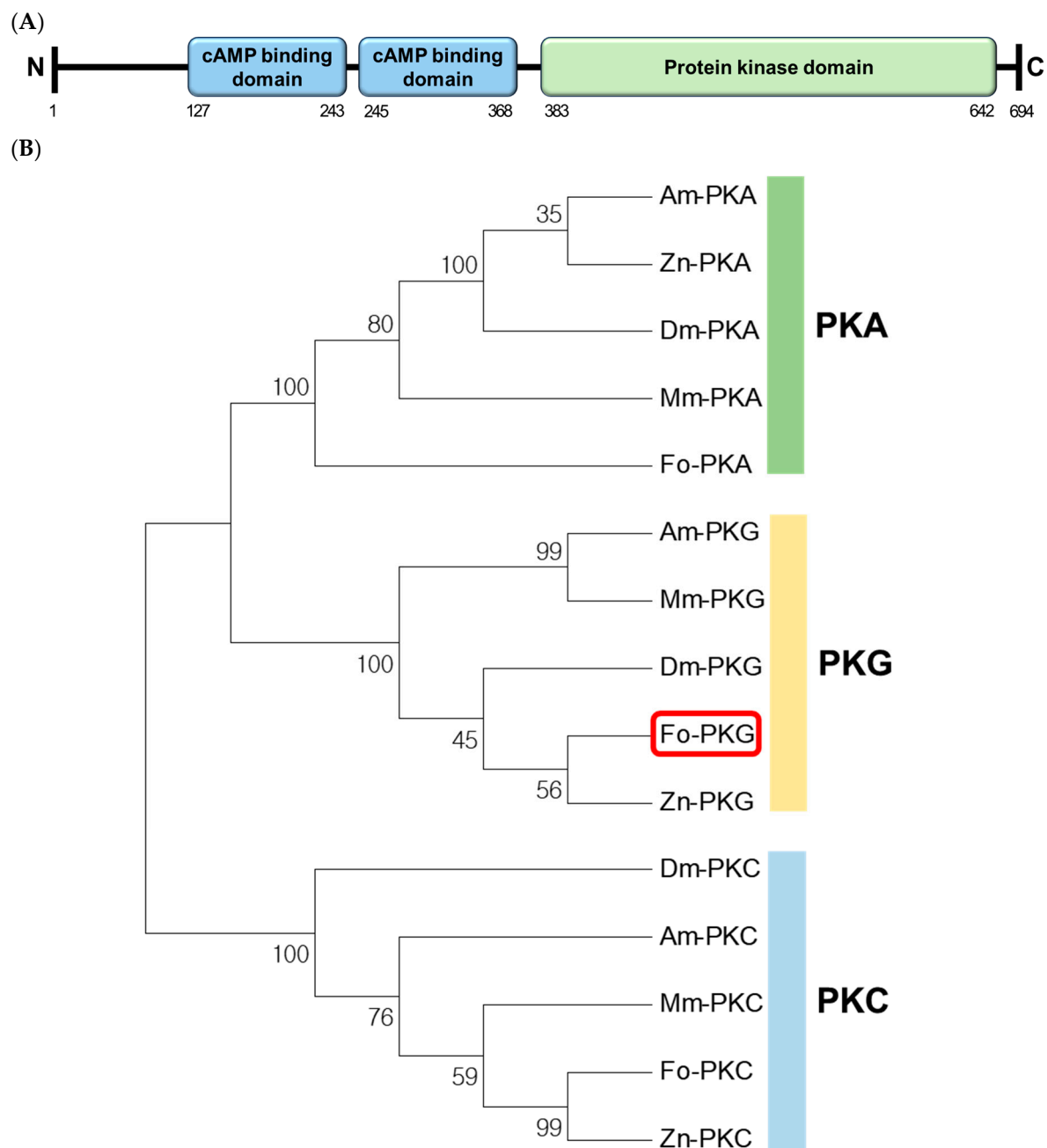
Percent data for genetic analyses were arcsine-transformed, and the subsequent transformed data were confirmed to follow a normal distribution using PROC UNIVARIATE of the SAS program [24]. Data obtained from the feeding or mating test were subjected to a one-way analysis of variance (ANOVA) using PROC GLM of the SAS program. The means were compared using the least significant difference (LSD) test at a Type I error of 0.05.

For behavioral monitoring, mean of each trial (four trials for dsCON and three trials for dsPKG) was measured initially. Subsequently means and standard deviations (SDs) of the trial means were obtained again as representative values of parameters and durations (%), according to the central limit theorem [25,26]. Considering high variability in behavioral data, Mann-Whitney U test was opted for analyzing nonparametric data (rank) while Kolmogorov-Smirnov test was additionally chosen for analyzing parametric data (mean and SD) concurrently (sample numbers with 96 and 72 for dsCON and dsPKG, respectively, for each parameter and duration (%)). The software was obtained from 'scipy.stats', a Python package (V1.14.1). By combining two test results, a statistical differentiation score was devised to indicate a possibility of quantitative separation between photo- and scoto-phases. Scores 1 and 2 were given to probability of alpha error less than 0.10 and 0.05 for each test, respectively. Then the scores for the two tests were summed to present overall statistical differentiation with maximum of 4 and minimum of 1. Additionally, the t-Test was conducted to compare parameters and durations (%) between dsCON and dsPKG directly in each light phase (four and three trials for ds CON and dsPKG, respectively, in each light phase) with one-tail analysis under the condition of heteroscedasticity, considering difference in variance between two treatments.

### 3. Results

#### 3.1. A PKG Gene Is Expressed in All Developmental Stages of *F. occidentalis*

A *Fo-PKG* gene (GenBank accession number: XM\_026417160.2) is encoded in the genome of *F. occidentalis* (Figure 1). It encodes an open reading frame translated into a sequence of 694 amino acids, which is predicted to have two cAMP binding domains and a protein kinase domain (Figure 1A). A phylogenetic tree indicates that *Fo-PKG* is clustered with other insects *PKG* genes but away from the gene clusters of *PKA* and *PKC* (Figure 1B). *Fo-PKG* was expressed in all developmental stages but exhibited relatively low expression level in pupal stage (Figure 1C). In young adults, both male and female had the highest expression levels of *Fo-PKG* at 3 days old after the emergence (Figure 1D). The expression levels abruptly reduced at old adults after 5 days after emergence.



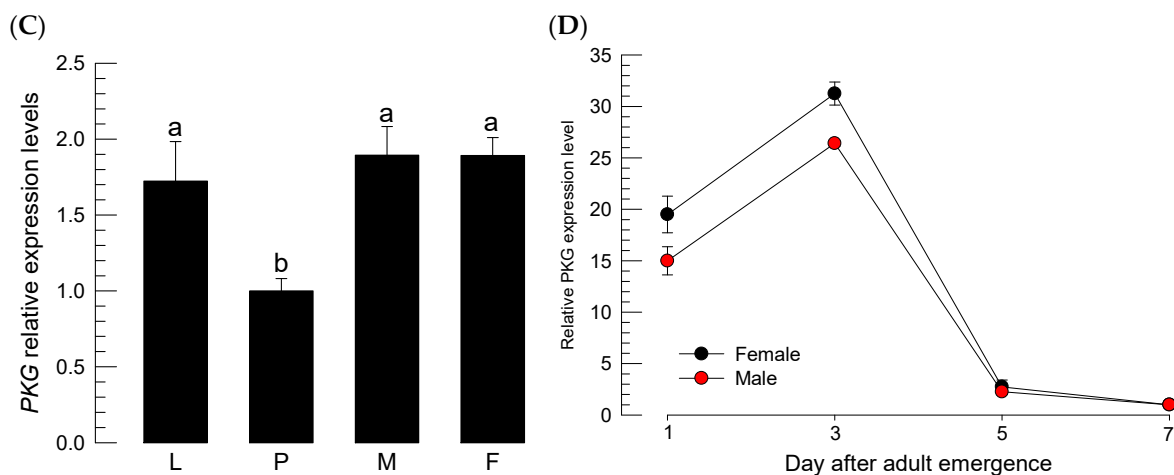
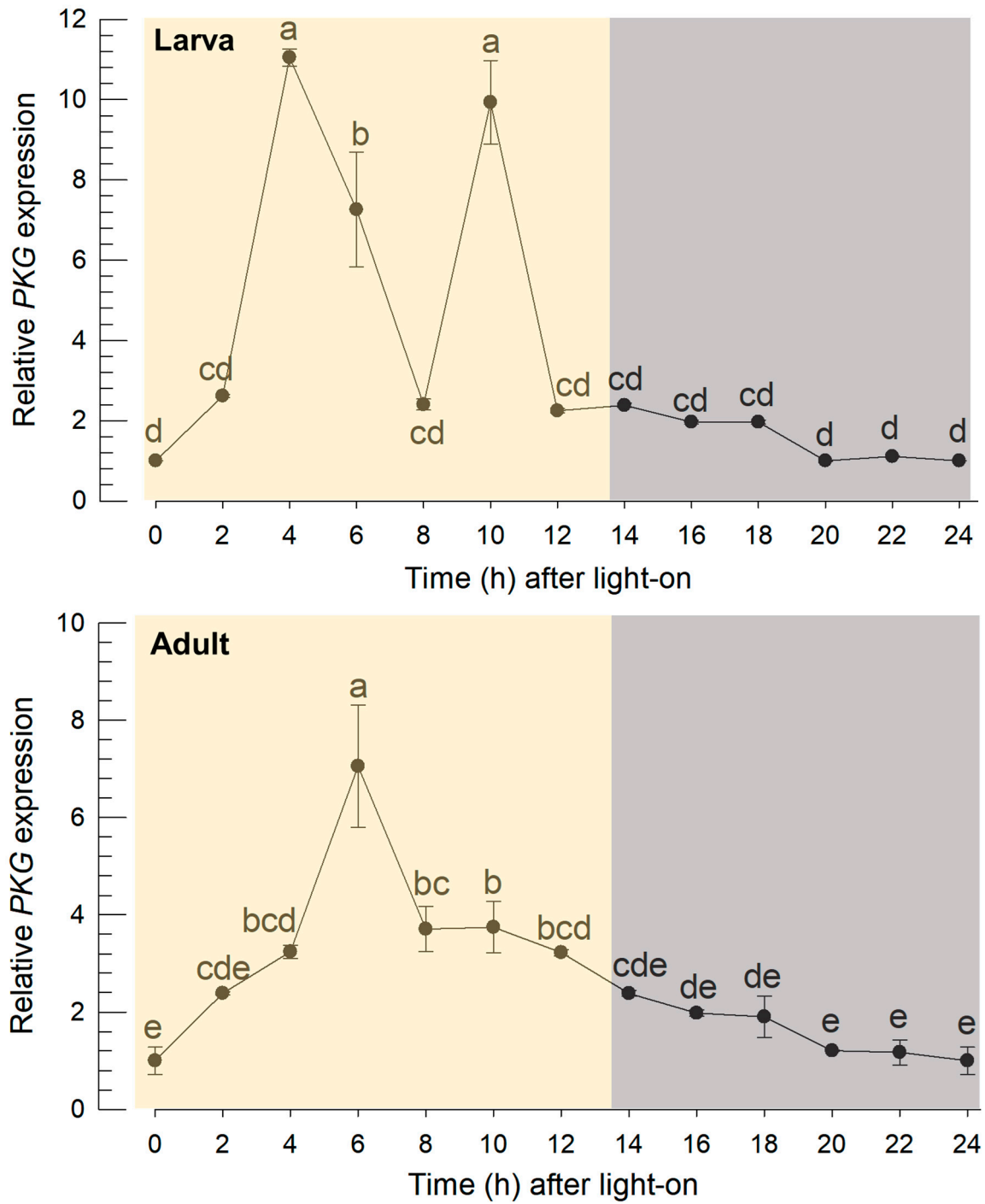


**Figure 1.** Molecular properties of *F. occidentalis* cGMP-dependent protein kinase (*Fo-PKG*). (A) Prediction of functional domains using Interpro (<http://www.ebi.ac.uk/interpro/>). Three domains are indicated on the amino acid sequence predicted from the open reading frame of *Fo-PKG*. (B) A phylogeny analysis of *Fo-PKG* with other PKG, cAMP-dependent protein kinase (*PKA*), and protein kinase C (*PKC*) genes using MEGA6. These genes are retrieved from GenBank with accession numbers of XP\_052121837.1 for *Fo-PKA*, NP\_476977.1 for *Drosophila melanogaster* PKA (*Dm-PKA*), XP\_393285.1 for *Apis mellifera* PKA (*Am-PKA*), XP\_021936510.1 for *Zootermopsis nevadensis* PKA (*Zn-PKA*), XP\_057317931.1 for *Microplitis mediator* PKA (*Mm-PKA*), XM\_026417160.2 for *Fo-PKG*, ACO44430.1 for *D. melanogaster* PKG (*Dm-PKG*), XP\_026300309.1 for *A. mellifera* PKG (*Am-PKG*), XP\_021933460.1 for *Z. nevadensis* PKG (*Zn-PKG*), XP\_057321318.1 for *M. mediator* PKG (*Mm-PKG*), XP\_052133408.1 for *F. occidentalis* PKC (*Fo-PKC*), NP\_001287577.1 for *D. melanogaster* PKC (*Dm-PKC*), XP\_026296808.1 for *A. mellifera* PKC (*Am-PKC*), XP\_021920016.1 for *Z. nevadensis* PKC (*Zn-PKC*), and XP\_057338986.1 for *M. mediator* PKC (*Mm-PKC*). (C) Expression profile of *Fo-PKG* in different developmental stages of larva (L), pupa (P), adult male (M), and adult female (F). (D) Change of expression levels of *Fo-PKG* in different adult ages. Expression level of an elongation factor, *Fo-EF1*, in each sample was used to normalize the expression level. In each treatment, three trials were used. Different letters above standard deviation bars indicate significant differences among means at Type I error = 0.05 (LSD test).

### 3.2. Diel Rhythmicity of *Fo-PKG* Expression Profile

To understand the diel rhythmicity of *Fo-PKG* expression, its expression levels were assessed every 2 h in a day (Figure 2A). In the larval stage, two expression peaks occurred at photophase, at which the overall gene expression levels were higher than those at scotophase ( $F = 95.10$ ,  $df = 1, 10$ ;  $P < 0.0001$ ). The high expression pattern at photophase was maintained in the adult stage with single high expression peak at 6 h after light-on. The overall expression levels during photophase were significantly ( $F = 82.43$ ,  $df = 1, 10$ ;  $P < 0.0001$ ) higher than those at scotophase in adult stage. The high expression of PKG gene at the photophase was visualized by FISH assay (Figure 2B). The fluorescence-labeled antisense probe specific to PKG mRNA specifically gave positive signal in the midgut of the adults at 6 h after light-on while its sense probe did not show any signal. However, the FISH signal was much weak in the midgut during scotophase, at which the normalized signal intensity was lower than that at the photophase by almost two folds.

(A)



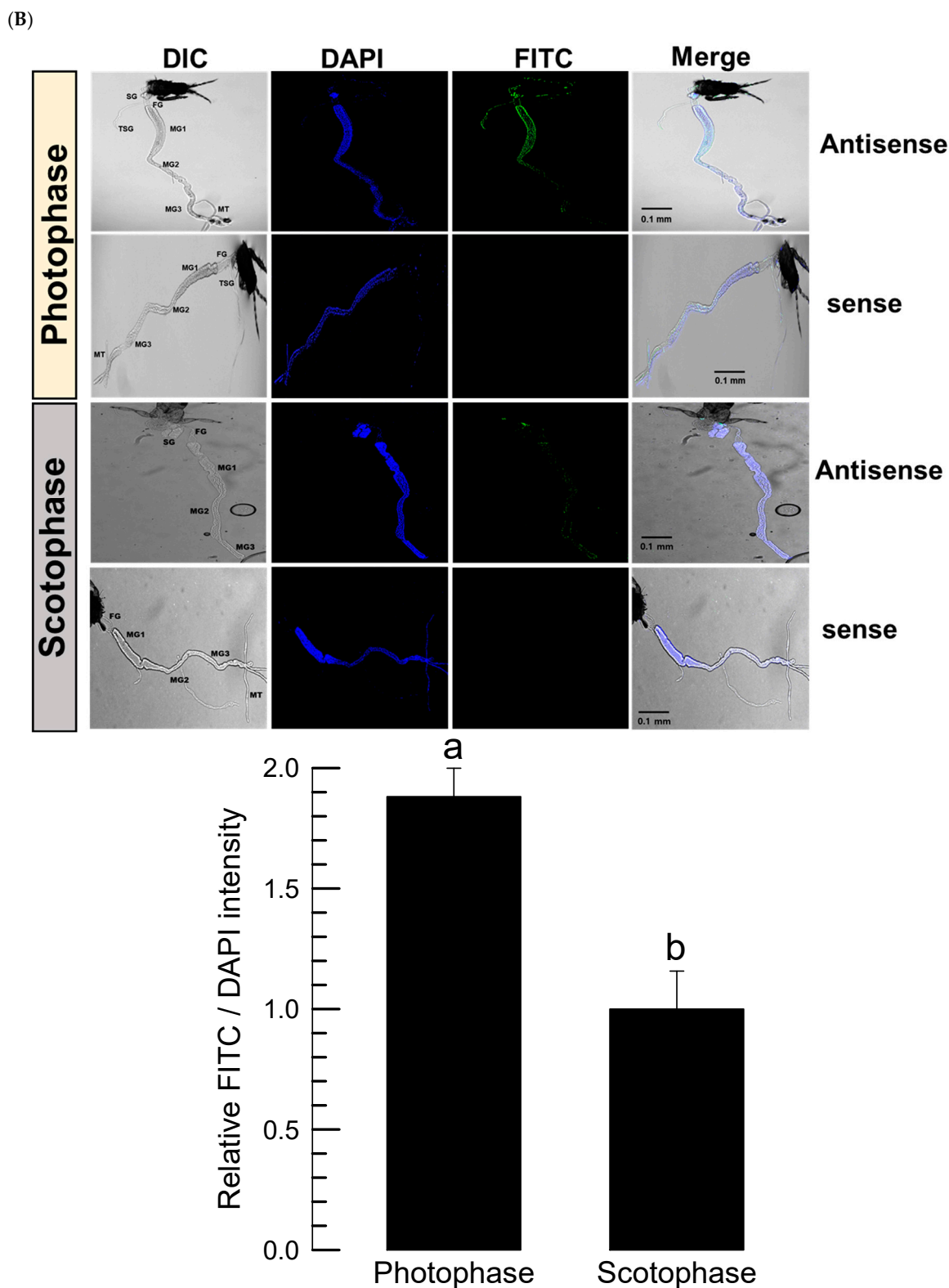


**Figure 2.** Diel rhythmicity of *PKG* expression in *F. occidentalis*. (A) RT-qPCR analysis of the gene every 2 h in larva and adult stages. Each measurement used 10 thrips and was independently repeated three times. Expression level of an elongation factor, *Fo-EF1*, was used to normalize the expression level. Different color backgrounds indicate photophase (0 ~ 14 h) and scotophase (14 ~ 24 h). (B) FISH analysis. Female adults were selected at photophase (6 h) and scotophase (18 h). Specific expression of *PKG* of *F. occidentalis* was observed with FITC-labeled antisense or sense probe. A fluorescent microscope (DM2500; Leica, Wetzlar, Germany) was used to view the samples in fluorescence ('FITC' against the probe and 'DAPI' against nucleus) while the intact morph was visualized in a mode of differential interference contrast (DIC) at 100x magnification. The scale bar

represents 0.1 mm. The intensity was quantified by normalizing the FITC and DAPI signals. Each treatment was replicated three times and each trial contained three female adults. Different letters above the standard deviation bars indicate significant differences between means at Type I error = 0.05 (LSD test).

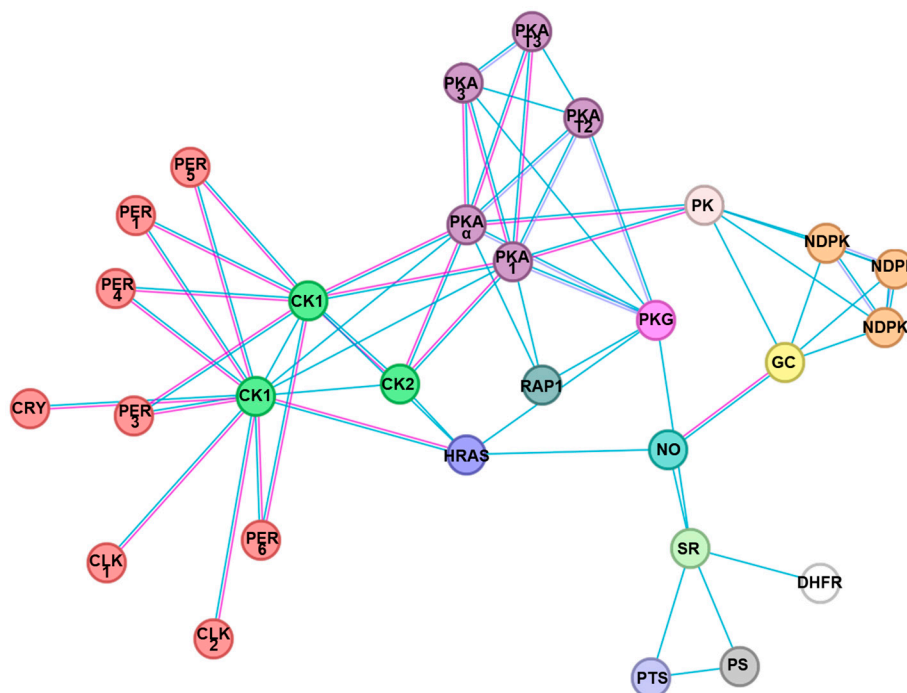
### 3.3. Functional Link Between PKG and Clock Genes

To predict a functional link of the expression of *Fo-PKG*, its protein-protein interactions were assessed using a String database (Figure 3A). This analysis indicated that PKG is directly linked with NO signaling as expected. Interestingly, PKG is linked to clock genes such as period (*Per*) and Clock (*CLK*) via casein kinase (*CK*) and cAMP-dependent protein kinase (*PKA*).

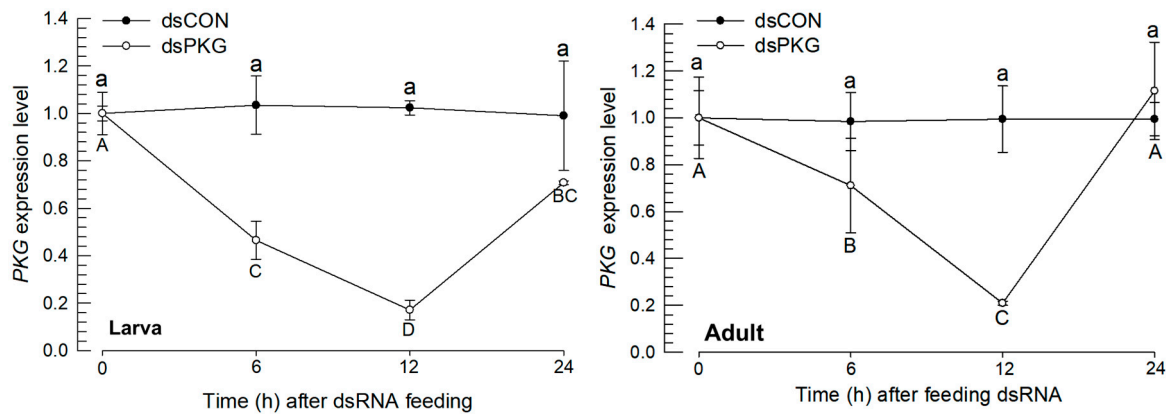
To investigate a functional association between PKG and the two clock genes, loss-of-function approach was applied by RNAi specific to *Fo-PKG*. Feeding dsPKG significantly suppressed the *Fo-PKG* expression in larvae and adults (Figure 3B). The RNAi effects were analyzed on the survival rate and reproduction rate of *F. occidentalis* (Figure S2). In the case of total thrips fed with dsPKG for 24 h, the survival rate decreased by approximately 20% starting from the third day (Figure S2A). Additionally, the oviposition rate showed a statistically significant decrease in the number of progenies laid per female when treated with dsPKG (Figure S2B). Thus, at least for one day after RNAi treatment, the thrips did not show any detrimental influence on the survival.

Under these RNAi conditions, the expressions of *CLK* and *Per* genes were assessed at two time points in each of photophase and scotophase (Figure 3C). The RNAi treatment against *Fo-PKG* expression significantly reduced the expressions of *CLK* and *Per* genes during photophase in both larvae and adult stages. However, the RNAi treatment did not influence on the clock gene expression during scotophase.

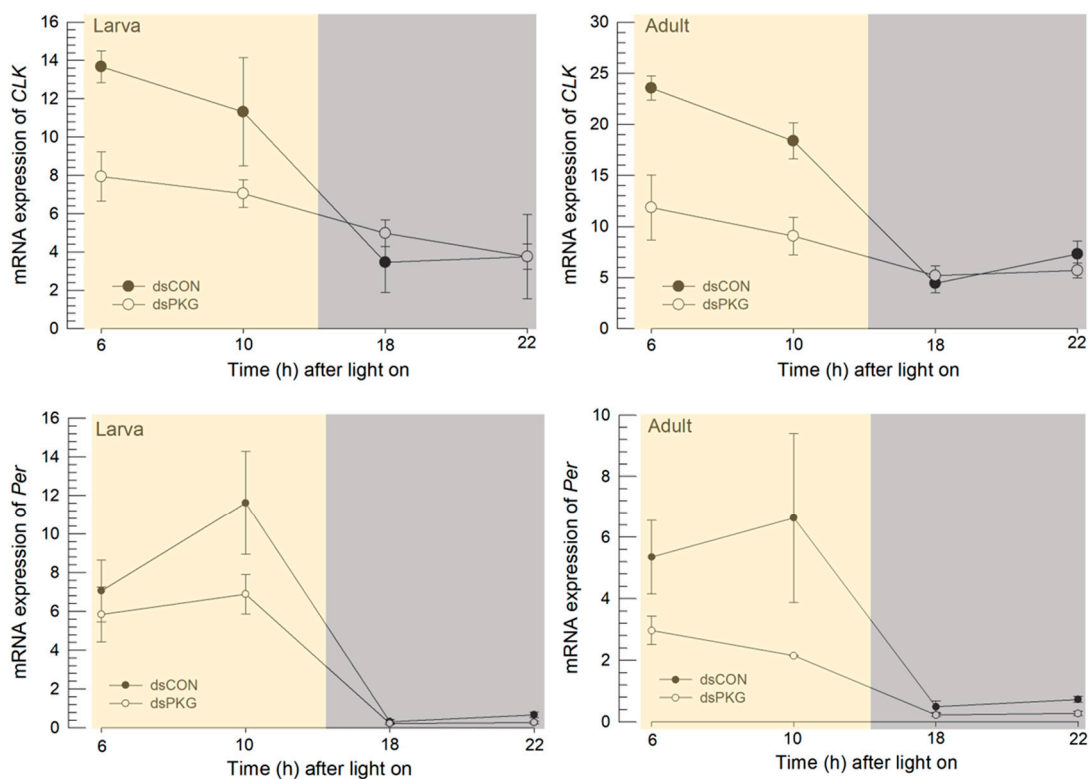
(A)



(B)



(C)



Gene	Stage	Time	$F$ (df = 1, 4)	$P$
<i>CLK</i>	Larva	Photophase	10.62	0.0100
		Scotophase	1.12	0.3152
	Adult	Photophase	20.64	0.0011
		Scotophase	0.15	0.7072
<i>Per</i>	Larva	Photophase	7.92	0.0183
		Scotophase	0.38	0.7990
	Adult	Photophase	30.22	0.0003
		Scotophase	0.81	0.3903

**Figure 3.** Functional association of PKG with clock genes in *F. occidentalis*. (A) A prediction of PKG interaction with other proteins: PKG (cGMP-dependent protein kinase), PER1 (Period circadian protein isoform X1), PER3 (Period circadian protein isoform X3), PER4 (Period circadian protein isoform X4), PER5 (Period circadian protein isoform X5), PER6 (Period circadian protein isoform X6), CLK1 (Circadian clock-dsCONled protein

daywake 1), CLK2 (Circadian clock-dsCONled protein daywake 2), CRY (Cryptochrome-1), CK1 (Casein kinase I subunit beta), CK2 (Casein kinase II subunit alpha), HRAS (GTPase HRas), RAP1 (Rap1 GTPase-activating protein 1), PKA $\alpha$  (cAMP-dependent protein kinase catalytic subunit alpha), PKA1 (cAMP-dependent protein kinase catalytic subunit 1), PKA3 (cAMP-dependent protein kinase catalytic subunit 3), PKAT2 (cAMP-dependent protein kinase type II regulatory subunit), PKAT3 (cAMP-dependent protein kinase type III regulatory subunit), PK (pyruvate kinase), NDPK (nucleoside diphosphate kinase), GC (guanylate cyclase), NO (nitric oxide synthase), SR (sepiapterin reductase), DHFR (dihydrofolate reductase), PTS (6-pyruvoyltetrahydropterin synthase), and PS (phosphodiesterase). The map was generated using STRING 12.0 (<https://string-db.org>). (B) RNAi efficacy of dsRNA feeding against *PKG* expression in *F. occidentalis*. Following dsPKG treatment, the expression levels of the *Fo-PKG* gene were assessed at different time points with 10 thrips per measurement. The qPCR was independently repeated three times. For dsCON, a nontarget gene, *EGFP*, was used for RNAi dsCON (dsCON). An elongation factor, *Fo-EF1*, was used to normalize the expression level. (C) Influence of RNAi specific to *PKG* expression on the expressions of clock genes: Clock (*Clk*) and Period (*Per*). After 24 h of dsPKG treatment, *CLK* and *Per* gene expressions were assessed at two-time points in each of photophase and scotophase.

### 3.4. Influence of the Reduced PKG Expression on Diel Rhythmicity of Adult Movement Behavior

Speed and locomotory rate in the total period were higher for dsCON ( $0.13 \pm 0.12$  mm/s) than those for dsPKG ( $0.07 \pm 0.07$  mm/s) (Table 1). DCR was overall similar between the two treatments. Durations (%) were substantially higher in the edge area (70.0 ~ 73.3 %) than the food-provision (13.3 ~ 18.4 %) and intermediate (8.3 ~ 16.7 %) areas in both treatments. It is noted that durations (%) in the intermediate area were higher for dsPKG (16.7 %) than for dsCON (8.3 %).

**Table 1.** Summary of movement parameters and durations (%) in different micro-areas in the observation arena for female thrips observed for 24 h continuously in dsCON and dsPKG.

Parameters		Treat. and Light phases		dsCON				dsPKG			
				Photophase		Scotophase		Photophase		Scotophase	
				Mean	SD	Mean	SD	Mean	SD	Mean	SD
Movement	Speed (mm/s)	0.16	0.13	0.08	0.08	0.07	0.07	0.06	0.07		
	Locomotory rate (mm/s)	0.17	0.13	0.08	0.09	0.07	0.07	0.06	0.07		
	DCR (°/s)	167.51	6.08	168.12	9.83	159.09	12.90	158.70	17.58		
Duration (%)	Food-provision	14.55	20.22	23.81	34.41	14.09	23.77	12.20	26.40		
	Intermediate	11.89	15.80	3.34	5.08	19.62	31.12	12.56	25.10		
	Edge	73.56	24.62	72.85	35.40	66.29	37.11	75.24	34.68		

Diel difference was observed with speed in dsCON with higher levels in photophase ( $0.16 \pm 0.13$  mm/s) than in scotophase ( $0.08 \pm 0.08$  mm/s) (Table 2). Locomotory rate was almost the same as the speed in photo- and scoto-phases. Diel difference was not observed in DCR in both treatments. It is noted that durations (%) in the intermediate area were higher in photophase than in scotophase in both treatments with 11.9 and 3.4, respectively, in dsCON, and 19.6 and 12.6, respectively, in dsPKG. Durations (%) in photo- and scoto-phases in both treatments were overall alike ranging 12.2 ~ 23.8 in the food-provision area and 66.3 ~ 75.2 in the edge area (Table 2).

**Table 2.** Movement parameters and durations (%) in different micro-areas in the observation arena for female thrips in photo- and scoto-phases observed for 24 h continuously in dsCON and dsPKG.

Parameters		Treat. and Light phases		dsCON				dsPKG			
				Photophase		Scotophase		Photophase		Scotophase	
				Mean	SD	Mean	SD	Mean	SD	Mean	SD
Movement	Speed (mm/s)	0.16	0.13	0.08	0.08	0.07	0.07	0.06	0.07		
	Locomotory rate (mm/s)	0.17	0.13	0.08	0.09	0.07	0.07	0.06	0.07		
	DCR (°/s)	167.51	6.08	168.12	9.83	159.09	12.90	158.70	17.58		
Duration (%)	Food-provision	14.55	20.22	23.81	34.41	14.09	23.77	12.20	26.40		
	Intermediate	11.89	15.80	3.34	5.08	19.62	31.12	12.56	25.10		
	Edge	73.56	24.62	72.85	35.40	66.29	37.11	75.24	34.68		

Behavior profiles across light phases were presented with speed superimposed over durations (%) as time progressed (Figure 4). Behavior patterns were divided into three consecutive stages in dsCON females. The stage started from the middle of the observation day for the convenience of comparison. The first stage included the changing phase from photophase to scotophase, P10 ~ S5, with maximal durations (%) in the edge area and minimal durations (%) in both food-provision and intermediate areas. The speed had a peak (0.25 mm/s) during P12 (arrow, Figure 4A), decreasing linearly afterward. In this stage, the females were not active in feeding and mainly moved around in the edge area especially in the initial period. In the second stage, S6 – S10, durations (%) in the food-provision area substantially increased to a maximal level (40.1 on average), indicating active feeding (Figure 4A). In the following third stage in photophase, P1 ~ P9, durations (%) in the intermediate areas (15.3 on average) were high, especially in P3 ~ P9, compared with the previous stages. Considering duration rates (%) in the food-provision (19.0 on average) and edge areas (65.7 on average) were also high, females moved around across different micro-area actively in this stage, partly involved in feeding. It is noted that speed was very high in the early photophase, P1 ~ P3, in this stage. This high speed may be due to the energy accumulated by feeding in the previous stage, S5 ~ S10 (Figure 4A).

Behavior profiles of the dsPKG (Figure 4B) were substantially different from those of dsCON. Overall, speed and durations (%) were irregular with intermittent peaks across light phases. In the initial stage, P10 ~ S5, durations (%) in the intermediate area substantially increased (41.6 on average), especially during P12 ~ S3. Three peaks of speed (0.10 ~ 0.13 mm/s) were also observed in this period. It is noted that durations (%) in the food-provision area were high in both beginning (P10 ~ P12) and end (S2 ~ S5) of this stage, indicating that the test females would be involved in feeding in these periods. Behaviors in the second stage in S6 ~ S10 were also contrastingly different from the control. The test females stayed in the edge area (81.5 % on average) almost the whole period, rarely visiting the food-provision area (13.3 % on average). Speed was in the intermediate range (0.05 mm/s on average) in this stage. In the third stage in photophase, P1 ~ P9, females variably visited different micro-areas with intermittently high levels of speed between 0.08 ~ 0.18 mm/s.



**Figure 4.** Durations (%) in micro-areas superimposed with speed of female thrips. (A) dsCON and (B) dsPKG.

The trends of movement parameters were compared between dsCON and dsPKG in detail in Figure 5. Diel difference in speed was observed with the dsCON females across light phases as stated above. The speed of the dsCON females was initially high at P1 (0.31 mm/s), remained in a low level (0.11 mm/s on average) during P5 ~ P8, and increased again from P9 to reach a peak at P12 (0.25 mm/s) (Figure 5A). Afterward, speed decreased continuously until S1 and was low almost through the whole period of scotophase (0.08 mm/s on average). For dsPKG-treated females, however, this type of diel difference was not observed with speed in consistently low levels (0.07 mm/s on average) throughout the observation period, except intermittently high levels between 0.13 ~ 0.18 mm/s. The trends of locomotory rate of dsCON and dsPKG were very similar to those of speed (Figure 5B), reflecting that the stops in movement did not much influence motility of test females measured with the time unit at 1 s. DCRs across light phases were overall stable in both dsCON and ds-PKG with relatively a higher degree of fluctuation observed in ds-PKG (Figure 5C).

Statistical significance was further obtained for comparing parameters between dsCON and dsPKG in each light phase according to t-Test (See Materials and methods). A few light phases showed the statistical differences. The speed showed significances mainly in late photophase, P9 – P11, between dsCON and dsPKG (Figure 5A). The light phases with alpha error up to 0.10 were also presented in the figure in P2 and P12. Locomotory rate had similar significance to the case of speed (Figure 5B). DCR had statistical significance during P2 and P10 with an alpha error, 0.05 (Figure 5C).

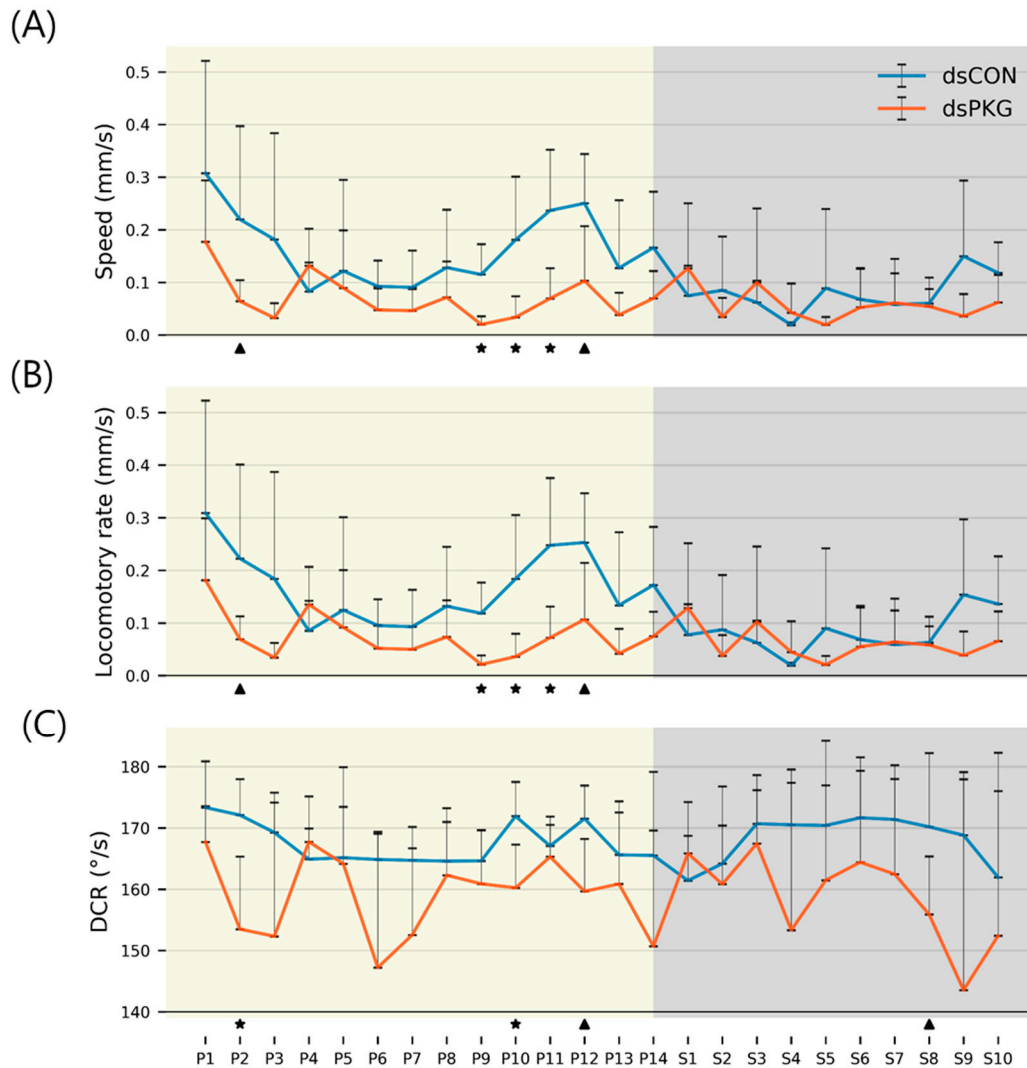


**Figure 5.** Movement parameters of female thrips. (A) Speed (B) Locomotory rate (C) Direction change rate (DCR) ('\*' alpha error up to 0.05 and '▲' alpha error up to 0.10 underneath each subfigure).

Durations (%) staying at the food area (Figure 6A) were initially similar between the treatments with low levels from early photophase to early scotophase (P1 ~ S2) (dsCON; 13.69% and dsPKG; 13.32%). Afterward, substantial differences between dsCON and dsPKG were observed in two phases. Early in S2 and S5, percentages staying in the food-provision area were higher with dsPKG (24.32 % on average) than dsCON (8.26% on average). Afterward from S6 to S10, reverse durations were observed with higher levels in dsCON (40.10% on average) and lower levels in dsPKG (4.72% on average).

In the intermediate area, durations (%) were characterized by an exceedingly high level for dsPKG during P12 ~ S2 (Figure 6B). Except for this, durations (%) were overall stable for dsCON and dsPKG at low levels. It is noted that SDs were exceptionally high with durations (%) for dsPKG in P12 ~ S2 (Figure 6B).

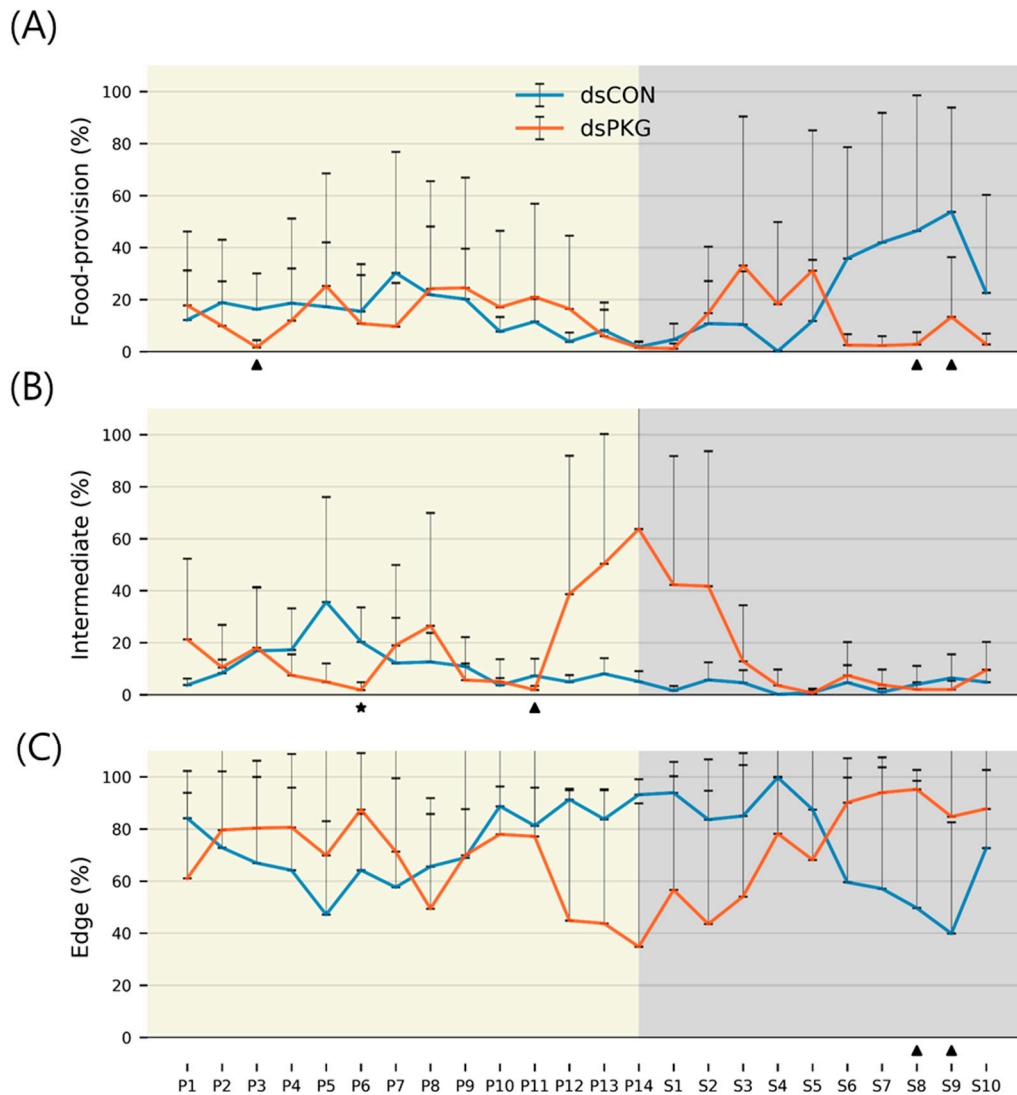


**Figure 6.** Durations (%) of female thrips staying in micro-areas. (A) Food-provision, (B) intermediate and (C) edge (\*' alpha error up to 0.05 and '▲' alpha error up to 0.10 underneath each subfigure).

Percentages of staying in the edge area (Figure 6C) were overall similar in early-to-mid photophase, P1 ~ P7, in dsCON (65.3% on average) and dsPKG (75.8% on average), although some levels of fluctuation were observed in both treatments during this phase. Subsequently, substantial differences were observed between dsCON and dsPKG in two phases. Early in P12 ~ S5, durations (%) were lower for dsPKG (53.00% on average) than for dsCON (89.75% on average). Afterward during S6 ~ S10, durations (%) were reversed, lower for dsCON (55.76% on average) than for dsPKG (90.36% on average). It is noted that the switching time for durations (%) was the same with S6 in both food-provision and edge areas (Figure 6A,C).

Durations (%) in different micro-areas between dsCON and dsPKG showed weak statistical significance compared with movement parameters (Figure 6). In the intermediate area, statistical significance was observed in one light phase, P6 (Figure 6B). The probability of alpha error up to 0.10 was only observed intermittently at a few light phases in the food-provision and edge areas (Figure 6A,C).

As shown in Figure 7, statistical differentiation scores were observed in speed and locomotory rate in dsCON especially with S4 vs most photophase with maximum scores equal to 4 (green arrows). Low degrees of differentiation with score 1 were also observed intermittently. In DCR, no meaningful statistical significance was observed. For dsPKG, speed and locomotory rate showed no statistical difference except for a few cases of intermittent differences with scores equal to 2, showing

only one test of statistical significance in these cases. In DCR, no difference was observed overall except one case (P1 vs P4) with the differentiation score equal to 2 in dsPKG treatment.

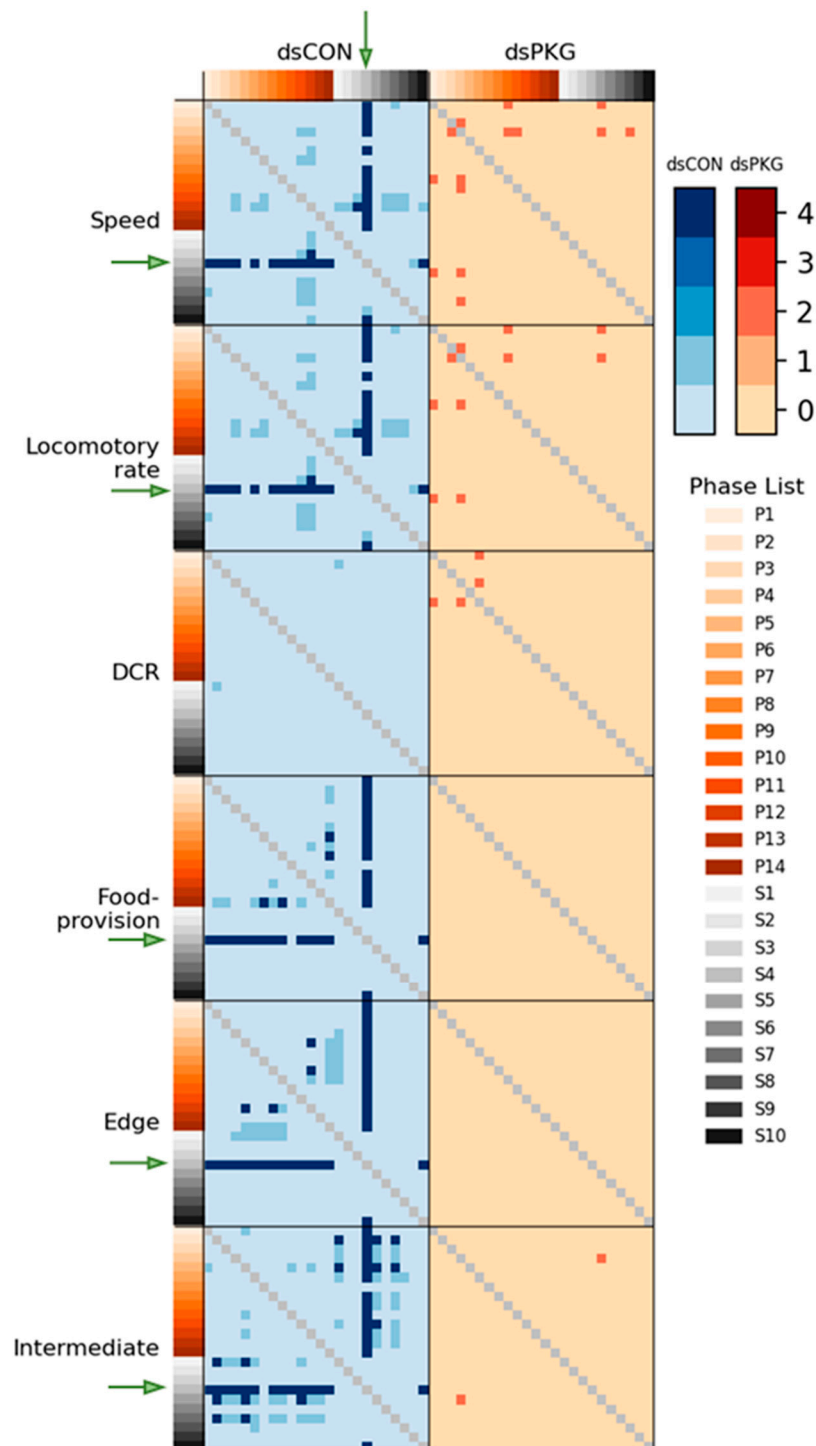


**Figure 7.** Statistical differentiation between dsCON and dsPKG in each hour phase in 24-h cycle according to combined results from Mann-Whitney U and Kolmogorov-Smirnov tests. (A) Movement parameters and (B) durations (%) in different micro-areas (Green arrows indicating S4).

Regarding durations (%) in the micro-areas, significances were also found with dsCON, more strongly in the intermediate area, while significances were not observed with dsPKG in all micro-areas (Figure 7). Like the cases of movement parameters, statistical differentiation of duration (%) was high in S4 vs most photophase with the scores equal to 4 with dsCON in all micro-areas (green arrows). Also in the intermediate area, maximum statistical differentiations with score equal to 4 were

found intermittently in P2, P5, S1, S5 and S7, along with minor differences with scored equal to 1. Intermittent statistical differentiations with score equal to 4 were found less in the food-provision and edge areas in photophase.

#### 4. Discussion

The continuous monitoring of the thrips behavior exhibited a diurnal rhythmicity by relatively high activity during photophase and relatively low activity during scotophase. This kind of the diel pattern is controlled by its circadian machinery equipped with two oscillatory loops: Per/TIM oscillatory loop and the CRY loop [27,28]. In each of these loops, CLK/CYC acts as a transcriptional activator that promotes *Per* and *TIM*, or *CRY* transcription. The product proteins Per and TIM, or CRY are thought to provide negative feedback to inhibit the transcriptional activator. In *D. melanogaster*, *CRY* is expressed in specific clock neurons in the brain [29]. *CRY* is then activated by blue light and catalyzes TIM degradation through its protease activity, at which point the circadian clock is reset [30,31]. In *F. occidentalis*, *Per* and *CLK* genes exhibited the diel patterns with relatively high expressions during photophase and relatively low expressions during scotophase. Interestingly, *PKG* expression followed this diel pattern, suggesting a functional association of its expression with the clock gene expressions.

RNAi specific to *PKG* expression led to alterations in the clock gene expressions during photophase by preventing up-regulation of the clock genes. *PKG* expression is associated with division of labor in honey bee, *Apis mellifera*, in which specific expression in the mushroom bodies of the brain, suboesophageal ganglion, and corpora allata is associated with foraging behavior to collect pollens and nectars [9]. The role of *PKG* expression in the labor division in social insects was also found in a fire ant, *Solenopsis invicta*, in which RNAi specific to *PKG* reduced the locomotory activity and facilitated the behavioral change from foragers to nurses [32]. *PKG* activity and locomotory activity has been well established in *Drosophila*, in which flies are discriminated into sitters with low *PKG* activity or rovers with high *PKG* activity [33]. These suggest that *PKG* expression is associated with high locomotory activities of *F. occidentalis* during photophase. Thus, the RNAi specific to *PKG* expression resulted in reduced immature development and adult fecundity presumably by inhibiting feeding and ovipositional behavior. In addition, the suppression of *PKG* expression led to the suppression of the clock gene expressions during photophase, supporting the functional association of the *PKG* expression with the circadian rhythmicity. In mammals, the suppression of clock gene expressions led to the suppression of *PKG* protein level [34]. This suggests that the alterations of the clock gene expressions may be indirect influence of the reduced *PKG* mRNA level caused by RNAi in *F. occidentalis*. The control of *PKG* level by the clock gene expressions needs to be addressed in future study. It is also noteworthy that there are at least four isoforms of *PKG* in *F. occidentalis* genome: 176 (XP\_052119469.1), 417 (XP\_052132331.1), 694 (XP\_026272945.1), and 1,010 (XP\_026272942.1) amino acid residues. In this study, we analyzed only *PKG* with 694 amino acid length isoform. Thus, the other isoforms should be analyzed in their independent roles.

Automatic individual recognition of alive individuals and continuous parameter extraction demonstrated movement behaviors of the thrips by *PKG* and associated clock genes. Diel rhythm in adult females with RNAi specific to *PKG* expression was substantially affected without showing much variation in the activity parameters and durations staying at different areas of observation arena, whereas the dsCON females showed clear diel difference.

The continuous detection of behaviors over entire period of 24 h effectively characterized diel difference between dsCON and dsPKG. Not only differences in movement parameters, but also differences in durations (%) in the micro-areas in the observation arena were observed between dsCON and dsPKG (see Table 1). It is noted that total speed was high (0.13 mm/s) in dsCON compared with dsPKG (0.07 mm/s), indicating high level of energy consumption by dsCON.

Behavior profiles were produced in three stages by superimposing speed over durations (%) on continuously observed data (see Figure 4). Overall, behavior profiles were effectively characterized by sequential stages, activity followed by feeding and visiting to other micro-areas in dsCON-

females, and corresponding behavior disruptions after dsPKG suppression (see Figure 4A,B). Currently, however, the causes of behavior profile changes are unknown. More studies are warranted regarding physiological and genetical aspects along with diverse experimental conditions in the future.

Although the means and SDs were highly variable in both movement parameters and durations (%), statistical significances according to Mann-Whitney U and Kolmogorov-Smirnov tests were found between photo- and scoto-phases in dsCON in both movement parameters and durations (%) in different micro-areas, whereas the difference was not observed in dsPKG (see Figure 7). It is noted that a period in scotophase, S4, mainly had statistical differentiations with most periods in photophase in both parameters and duration rates (%) in dsCON, confirming coincidence in movement parameters and durations (%) in behavioral changes. The phase, S4 in mid-scotophase, had the minimum speed (0.19 mm/s) and locomotory rate (0.19 mm/s) along with minimal SD ranges (see Figure 5A,B). Similarly, durations (%) in S4 were either maximal in the edge area or minimal in the food-provision and intermediate areas, while SDs were commonly minimal in this phase (see Figure 6). The distinctive differences in mean values between light phases, concurrently with minimal range in SDs, contributed to presenting statistical significance originating from S4 in light phases.

Statistical significance of parameters was also examined specifically between dsCON and dsPKG in each light phase according to t-Test (See Materials and methods). The speed and locomotory rate showed significance mainly in three light phases, P9 – P11, between dsCON and dsPKG (see Figure 5A,B). These differences were contrasted with the case of statistical differences within each treatment where S4 was different from photophase as stated above (see Figure 7). The results suggested two aspects in behavioral changes: the late photophase was more discernable in comparing dsCON and dsPKG effects in each light phase, while the light phase S4 would be more affected after dsPKG suppression in relating with other light phases. Since high variability existed in the behavioral data, results need to be confirmed with more investigations through integrative approaches linking behavior, physiology and genetics along with more trials.

It is noted that the intermediate area played an important role in presenting behavioral changes. Duration increased to 16.7% for dsPKG while it was low with 8.3% for dsCON (see Table 1). In addition, the tested females in the intermediate area had high duration in photophase (11.9%) compared with scotophase (3.3%) in dsCON (see Table 2). This suggested female activities could be more sensitively presented in the intermediate area in open space within the observation arena. It is also noteworthy that the tested females stayed a long time in the edge area (70.0 ~ 73.3%) compared with other micro-areas in both treatments (e.g., Table 1). This may indicate that the tendency staying near boundary would persist after PKG modulation.

Durations (%) were extremely high during P12 ~ S2 compared with other light phases in dsPKG (see Figure 7). However, no distinctive statistical differentiation was observed among light phases on duration (%) in the intermediate area in dsPKG. This would be due to the extremely high levels of SDs of durations (%) observed in this period, P12 ~ S2. Further physiological and genetical investigations are required along with more trials to confirm if diel differences would exist in durations (%) in the intermediate area in dsPKG

During P1, very high speed was observed in both treatments (see Figure 5A). This would present high activity after feeding in the previous stage in photophase (see Figure 4A) as discussed above. But the speed was also high in P1 for dsPKG, although feeding did not occur in the previous stage for dsPKG (see Figure 4B). More investigations are required in the future regarding examinations of mechanisms causing high speed in P1 in dsPKG or effect of acclimation to initial behavior in the observation arena.

With continuous observation of movement activity and visiting places at the same time, the computational analysis of response behaviors supported physiological evidences of dsPKG suppression effects, demonstrating changes in behavioral status according to instantaneous movement parameters and durations (%) in different micro-areas, and revealing consecutive behavioral changes as well. Further study on reasonable guidance for molecular physiological

approach to behavioral data is warranted in the future in illustrating genetic functioning in an integrated manner.

**Supplementary Materials:** The following supporting information can be downloaded at the website of this paper posted on Preprints.org, Figure S1: Observation of continuous movement of *F. occidentalis* under the conditions described below. (A) Observation system. (B) Micro-areas in the observation arena (top view). (C) Observation arena with food and water supply (side view). (D) An example of movement tracks in photo- and scoto-phases.; Figure S2: Influence of PKG suppression by its specific RNAi on immature development (A) and adult fecundity (B) in *F. occidentalis*. Test thrips were fed with dsRNA specific to PKG ('dsPKG') at 500 µg/mL for 24 h. For dsCON, a nontarget gene, *EGFP*, was used for RNAi dsCON ('dsCON'). Each treatment was replicated three times. Different letters above standard deviation bars indicate significant differences among means at Type I error = 0.05 (LSD test).; Table S1: Primers used in this study and their PCR conditions.

**Author Contributions:** Conceptualization, Y.K. and T.C.; methodology, G.J., F.K., H.K., Y.J., N.J. and C.X.; software, G.J., F.K., H.K., Y.J., N.J. and C.X.; validation, G.J., F.K., H.K., Y.J., N.J. and C.X.; formal analysis, G.J., F.K., H.K., Y.J., N.J. and C.X.; investigation, G.J., F.K., H.K., Y.J., N.J., C.X., Y.K. and T.C.; resources, Y.K. and T.C.; data curation, G.J., F.K., H.K., Y.J., N.J. and C.X.; writing—original draft preparation, Y.K. and T.C.; writing—review and editing, Y.K. and T.C.; visualization, G.J., F.K., H.K., Y.J., N.J. and C.X.; supervision, Y.K. and T.C.; project administration, Y.K. and T.C.; funding acquisition, Y.K. and T.C. All authors have read and agreed to the published version of the manuscript.

**Funding:** This work was supported by two grants (No. 2022R1A2B5B03001792 and No. 2022R1A2C1092725) of the National Research Foundation (NRF) funded by the Ministry of Science, ICT and Future Planning, Republic of Korea. This work was also supported by another grant from NRF funded by the Korea government (MSIT) (RS-2022-NR069997).

**Data Availability Statement:** Protein sequences are found in GenBank under the accession numbers given in the caption of Figure 1.

**Acknowledgments:** We appreciate Youngim Song in Andong National University for her supplying test compounds and other materials.

**Conflicts of Interest:** The authors declare no conflict of interest.

## References

1. Kim, C.Y.; Choi, D.Y.; Kang, J.H.; Ahmed, S.; Kil, E.J.; Kwon, G.M.; Lee, G.S.; Kim, Y. Thrips infesting hot pepper cultured in greenhouses and variation in gene sequences encoded in TSWV. *Korean J. Appl. Entomol.* **2021**, *60*, 381-401.
2. Rotenberg, D.; Jacobson, A.L.; Schneweis, D.J.; Whitfield, A.E. Thrips transmission of tospoviruses. *Curr. Opin. Virol.* **2015**, *15*, 80-89.
3. He, Z.; Guo, J.F.; Reitz, S.R.; Lei, Z.R.; Wu, S.Y. A global invasion by the thrips, *Frankliniella occidentalis*: current virus vector status and its management. *Insect Sci.* **2020**, *27*, 626-645.
4. Reitz, S.R.; Gao, Y.; Kirk, W.D.J.; Hoddle, M.S.; Leiss, K.A.; Funderburk, J.E. Invasion biology, ecology, and management of western flower thrips. *Annu. Rev. Entomol.* **2020**, *65*, 17-37.
5. Sampson, C.; Kirk, W.D. Can mass trapping reduce thrips damage and is it economically viable? Management of the Western flower thrips in strawberry. *PLoS ONE* **2013**, *8*, e80787.
6. Kim, C.Y.; Khan, F.; Kim, Y. A push-pull strategy to dsCON the western flower thrips, *Frankliniella occidentalis*, using alarm and aggregation pheromones. *PLoS ONE* **2023**, *18*, e0279646.
7. Ren, X.; Wu, S.; Xing, Z.; Xu, R.; Cai, W.; Lei, Z. Behavioral responses of western flower thrips (*Frankliniella occidentalis*) to visual and olfactory cues at short distances. *Insects* **2020**, *11*, 177.
8. Kim, C.; Akter, S.; Kim, Y. Diel rhythm of feeding and mating behaviors of the western flower thrips, *Frankliniella occidentalis*. *Proc. Natl. Acad. Sci. ROK* **2023**, *62*, 567-596.
9. Thamm, M.; Scheiner, R. PKG in honey bees: spatial expression, *Amfor* gene expression, sucrose responsiveness, and division of labor. *J. Comp. Neurol.* **2014**, *522*, 1786-1799.

10. Reaume, C.J.; Sokolowski, M.B. cGMP-dependent protein kinase as a modifier of behaviour. *Handb. Exp. Pharmacol.* **2009**, *191*, 423-443.
11. Lucas, C.; Ben-Shahar, Y. The foraging gene as a modulator of division of labour in social insects. *J. Neurogenet.* **2021**, *35*, 168-178.
12. Allen, A.M.; Sokolowski, M.B. Expression of the foraging gene in adult *Drosophila melanogaster*. *J. Neurogenet.* **2021**, *35*, 192-212.
13. Ben-Shahar, Y. The foraging gene, behavioral plasticity, and honeybee division of labor. *J. Comp. Physiol. A* **2005**, *191*, 987-994.
14. Tobback, J.; Mommaerts, V.; Vandersmissen, H.P.; Smagghe, G.; Huybrechts, R. Age- and task-dependent foraging gene expression in the bumblebee *Bombus terrestris*. *Arch. Insect Biochem. Physiol.* **2011**, *76*, 30-42.
15. Plano, S.A.; Alessandro, M.S.; Trebuçq, L.L.; Endo, S.; Golombek, D.A.; Chiesa, J.J. Role of G-substrate in the NO/cGMP/PKG signal transduction pathway for photic entrainment of the hamster circadian clock. *ASN Neuro.* **2021**, *13*, 1759091420984920.
16. Bustin, S.A.; Benes, V.; Garson, J.A.; Hellemans, J.; Huggett, J.; Kubista, M.; Mueller, R.; Nolan, T.; Pfaffl, M.W.; Shipley G.L.; et al. The MIQE guidelines: minimum information for publication of quantitative real-time PCR experiments. *Clin. Chem.* **2009**, *55*, 611-622.
17. Livak, K.J.; Schmittgen, T.D. Analysis of relative gene expression data analysis using real-time quantitative PCR and the  $2^{-\Delta\Delta CT}$  method. *Methods* **2001**, *25*, 402-408.
18. Vatanparast, M.; Ahmed, S.; Herrero, S.; Kim, Y. A non-venomous sPLA<sub>2</sub> of a lepidopteran insect: Its physiological functions in development and immunity. *Dev. Comp. Immunol.* **2018**, *89*, 83-92.
19. Akinyemi, A.O.; Subramanian, S.; Mfuti, D.K.; Pope, T.W.; Tamiru, A.; Kirk, W.D.J. Mating behaviour, mate choice and female resistance in the bean flower thrips (*Megalurothrips sjostedti*). *Sci. Rep.* **2021**, *11*, 14504.
20. Solawetz, J.F. What is YOLOv8? The Ultimate Guide. Blog post. <https://blog.roboflow.com/whats-new-in-yolov8>, 2023.
21. Choi, K.H.; Kim, J.S.; Kim, Y.S.; Yoo, M.A.; Chon, T.S. Pattern detection of movement behaviors in genotype variation of *Drosophila melanogaster* by using self-organizing map. *Ecol. Inform.* **2006**, *3*, 219-228.
22. Liu, Y.; Chon, T.S.; Baek, H.; Do, Y.; Choi, J.H.; Chung, Y.D. Permutation entropy applied to movement behavioral of *Drosophila melanogaster*. *Mod. Phys. Lett. B* **2011**, *25*, 1133-1142.
23. Eom, H.J.; Liu, Y.; Kwak, G.S.; Heo, M.; Song, K.S.; Chung, Y.D.; Chon, T.S.; Choi, J. Inhalation toxicity monitoring of indoor air pollutants in *Drosophila melanogaster* using integrated transcriptomics and computational behavior analyses. *Sci. Rep.* **2017**, *7*, 46473.
24. SAS Institute Inc. SAS/STAT user's guide, Release 6.03, Ed. Cary, NC, 1989.
25. Fischer, H. A history of the central limit theorem: from classical to modern probability theory. Vol. 4, Springer, New York, 2011.
26. Kwak, S.G., Kim J.H. Central limit theorem: the cornerstone of modern statistics. *Korean J. Anesthesiol.* **2017**, *70*, 144-156.
27. Tokuoka, A.; Itoh, T.Q.; Hori, S.; Uryu, O.; Danbara, Y.; Nose, M.; Bando, T.; Tanimura, T.; Tomioka, K. cryptochrome genes form an oscillatory loop independent of the per/tim loop in the circadian clockwork of the cricket *Gryllus bimaculatus*. *Zool. Lett.* **2017**, *3*, 5.
28. Tomioka, K., Matsumoto, A. The circadian system in insects: cellular, molecular, and functional organization. *Adv. Insect Physiol.* **2019**, *56*, 73-115.
29. Emery, P.; Stanewsky, R.; Hall, J.C.; Rosbash, M. *Drosophila* cryptochromes: a unique circadian-rhythm photoreceptor. *Nature* **2000**, *404*, 456-457.
30. Lee, C.; Parikh, V.; Itsukaichi, T.; Bae, K.; Edery, I. Resetting the *Drosophila* clock by photic regulation of PER and a PER-TIM complex. *Science* **1996**, *271*, 1740-1744.
31. Ceriani, M.F.; Darlington, T.K.; Staknis, D.; Mas, P.; Petti, A.A.; Weitz, C.J.; Kay, S.A. Light-dependent sequestration of TIMELESS by CRYPTOCHROME. *Science* **1999**, *285*, 553-556.
32. Chen, J.; Zhou, Y.; Lei, Y.; Shi, Q.; Qi, G.; He, Y.; Lyu, L. Role of the foraging gene in worker behavioral transition in the red imported fire ant, *Solenopsis invicta* (Hymenoptera: Formicidae). *Pest Manag. Sci.* **2022**, *78*, 2964-2975.

33. Osborne, K.A.; Robichon, A.; Burgess, E.; Butland, S.; Shaw, R.A.; Coulthard, A.; Pereira, H.S.; Greenspan, R.J.; Sokolowski, M.B. Natural behavior polymorphism due to a cGMP-dependent protein kinase of *Drosophila*. *Science* **1997**, *277*, 834-836.
34. Che, Y.; Shimizu, Y.; Hayashi, T.; Suzuki, J.; Pu, Z.; Tsuzuki, K.; Narita, S.; Shibata, R.; Murohara, T. Chronic circadian rhythm disorder induces heart failure with preserved ejection fraction-like phenotype through the Clock-sGC-cGMP-PKG1 signaling pathway. *Sci. Rep.* **2024**, *14*, 10777.

**Disclaimer/Publisher's Note:** The statements, opinions and data contained in all publications are solely those of the individual author(s) and contributor(s) and not of MDPI and/or the editor(s). MDPI and/or the editor(s) disclaim responsibility for any injury to people or property resulting from any ideas, methods, instructions or products referred to in the content.